Atomic Data and Nuclear Data Tables 120 (2018) 323–337

Contents lists available at ScienceDirect

Atomic Data and Nuclear Data Tables

journal homepage: www.elsevier.com/locate/adt

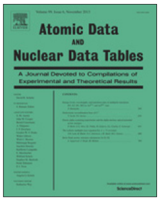

Second spectrum of Chromium (Cr II), Part II: Radiative lifetimes and oscillator strengths of transitions depopulating low lying $3d^44p$ levels

Safa Bouazza [a,*], Pascal Quinet [b,c], Patrick Palmeri [b]

[a] *Département de Physique, Université de Reims–Champagne, UFR SEN, BP 1039 F-51687 Reims Cedex2, France*
[b] *Physique Atomique et Astrophysique, Université de Mons-UMONS, B-7000 Mons, Belgium*
[c] *IPNAS, Université de Liège, B-4000 Liège, Belgium*

ARTICLE INFO

Article history:
Received 2 May 2017
Received in revised form 22 May 2017
Accepted 28 May 2017
Available online 20 June 2017

ABSTRACT

Radiative lifetime and oscillator strength values were computed by means of a pseudo-relativistic Hartree–Fock model including core-polarization and compared successfully with experimental data given in the literature for respectively numerous low-lying Cr II $3d^44p$ levels, up to 54784 cm^{-1}, and transitions depopulating these levels. Then transition probability and branching fraction data were also deduced in the wavelength range 1825–94400 Å. Furthermore the extracted radial integral values, obtained with the help of the oscillator strength parameterization method, are given for involved transitions in this work, i.e. $3d^44s$–$3d^44p$, $3d^5$–$3d^44p$ and $3d^44p$–$3d^44d$. We confirm our observed previous general trends, noting once again a decreasing of transition radial integral values with filling nd shells of the same principal quantum numbers for $nd^k(n+1)s \rightarrow nd^k(n+1)p$ transitions.

---

* Corresponding author.
E-mail address: safa.bouazza@univ-reims.fr (S. Bouazza).

http://dx.doi.org/10.1016/j.adt.2017.05.008

Contents

1. Introduction

The importance of accurate wavelengths and level energy values is now highly recognized in atomic physics when studying hyperfine structure, isotope shifts, oscillator strengths or transition probabilities of (sometimes blended) stellar spectral lines. It is particularly difficult to disentangle the blends, in the case of the elements of the 3d group due to their high relative abundance and line-rich spectra. Fortunately now we have the chance to go through high resolution spectra recorded with Fourier Transform spectrometers (FTS) which have the potential to improve significantly the accuracy of the first-given wavelengths and then the precision of energy levels by at least an order of magnitude. For Cr II the most recent complete compilation of energy level data is that of Sugar & Corliss [1], based on the analysis of Kiess [2] who reported for the first time observations of spectra excited in direct current arcs and condensed sparks between chromium electrodes. The latter author succeeded in classifying 1843 lines linking 138 even-parity levels of $3d^5$, $3d^4 4s$ and $3d^3 4s^2$ configurations with 139 $3d^4 4p$ odd-parity levels. Johansson et al. [3] extended the Kiess study a half century later, particularly in the near-infrared region and analyzed 450 additional levels. Sansonetti et al. [4–6] reported in turn new observations of Cr II some years later, in the near-ultraviolet region 1140–3400 Å, and also up to the infrared region: 2850–37900 Å, using a 10.7 m normal incidence spectrograph and an FT700 vacuum ultraviolet Fourier transform spectrometer. These new measurements have been used to revise most of the Cr II known levels [5–8]. These reanalyzes have permitted to exchange assignments of some levels classified in earlier lists of energy levels, to shift positions of some quartets like $3d^4 5d\ ^4F_J$ for instance and to predict some still missing energy levels. In our previous works, when determining radiative parameter values of some ions we have observed as general trends a decreasing of transition radial integral values with filling nd-shells of the same principal quantum numbers for $nd^k(n+1)s \rightarrow nd^k(n+1)p$ transitions. In the present work one of our aims is to extend the study of transition radial integral behavior to another ion, located in the same row of the periodic Table, namely Cr II, and by the way to check our predicted transition radial integral value given in [9]. To extract this latter value we can take advantage of experimental oscillator strengths or transition probabilities, plentifully available in literature [10–14].

2. Oscillator strength calculations

2.1. Some reminders

We open this paragraph by reminding the reader of important relations we have made use in this work, split in several parts dealing each one with particular transitions: $3d^4 4s$–$3d^4 4p$, $3d^4 4p$–$3d^4 5s$, $3d^4 4p$–$3d^4 4d$, ... The oscillator strength $f(\gamma\gamma')$ for the transition between two levels $|\gamma J\rangle$ and $|\gamma' J'\rangle$ of an atom or molecule with statistical weights $g = (2J+1)$ and $g' = (2J'+1)$ respectively, is a dimensionless physical quantity, expressing the probability of absorption or emission in this transition between these two levels and related to the transition probability $W(\gamma\gamma')$ by work [15]

$$W(\gamma\gamma') = \frac{2\omega^2 e^2}{mc^2} f(\gamma\gamma') \tag{1}$$

where m and e are the electron mass and charge, c is the velocity of light, γ describes the initial quantum state, $\omega = \frac{E(\gamma)-E(\gamma')}{\hbar}$, $E(\gamma)$ is the energy of the initial state. The quantities with primes refer to the final state. For the electric dipole transitions, the weighted oscillator strength gf is related to the line strength S [15]

$$gf = 8\pi^2 mca_0^2 \frac{\sigma}{3h} S = 303.76 \times 10^{-8} \sigma S \tag{2}$$

where a_0 is the Bohr radius, $\sigma = \frac{E(\gamma)-E(\gamma')}{hc}$ and h is Planck's constant. The electric dipole line strength is defined by

$$S = |\langle \gamma J \| P^1 \| \gamma' J' \rangle|^2. \tag{3}$$

This quantity is a measure of the total strength of the spectral line, including all possible transitions. The tensorial operator P^1 (first order) given in units of ea_0 in the reduced matrix element stands for the electric dipole moment. To obtain the gf value, we need to calculate initially S, or preferably its square root. For multiconfiguration systems, the wavefunctions $|\gamma J\rangle$ and $|\gamma' J'\rangle$ are expanded in terms of a set of basis functions $|\phi SLJ\rangle$ and $|\phi' S'L'J'\rangle$, respectively

$$\begin{aligned} |\gamma J\rangle &= \sum_i c_i\ |\phi_i S_i L_i J\rangle \\ |\gamma' J'\rangle &= \sum_j c'_j\ |\phi'_j S'_j L'_j J'\rangle. \end{aligned} \tag{4}$$

The square root of the line strength may be written in the following form

$$S^{1/2}_{\gamma\gamma'} = \sum_i \sum_j c_i c_j \langle \phi_i S_i L_i J \| P^1 \| \phi'_j S'_j L'_j J' \rangle . \tag{5}$$

In this work we have recurred to the eigenvector amplitudes obtained by a parametric analysis of multiconfiguration systems of Cr II reported in our previous paper [8].

The even system contains 11 configurations: $3d^5$ + $3d^4ns$ ($n = 4-9$) + $3d^4n'd$ ($n' = 4-6$) + $3d^34s^2$, and the odd system contains 6 configurations: $3d^44p + 3d^45p + 3d^46p + 3d^34s4p + 3d^44f + 3d^45f$. The appropriate computer program [16] calculates the angular part of the matrix element $\langle \phi SLJ \| P^1 \| \phi' S' L' J' \rangle$. From Eqs. (2) and (5), we can express the *gf*-values as a linear combination

$$(gf)^{1/2} = \sum_{nl,n'l'} (303.76 \times 10^{-8}\sigma)^{1/2} \times \sum_i \sum_j c_i c'_j \langle \phi_i S_i L_i J \| P^1 \| \phi'_j S'_j L'_j J' \rangle \tag{6}$$

where σ is the wavenumber, given in cm^{-1}, and the sum extends over all possible transitions ($ns \leftrightarrow n'\text{p}$, $nd \leftrightarrow n'\text{p}$, $nd \leftrightarrow n'\text{f}$). The probability per unit time of an atom in a specific state γJ to make a spontaneous transition to any state with lower energy is $P(\gamma J) = \sum A(\gamma J, \gamma' J')$, where $A(\gamma J, \gamma' J')$ is the Einstein spontaneous emission transition probability rate for a transition from γJ to $\gamma' J'$ states. The sum is over all $\gamma' J'$ states with $E(\gamma' J') < E(\gamma J)$.

The weighted transition probability is [17]

$$gA = (2J' + 1)A = \frac{64\pi^4 e^2 a_0}{3h}\sigma^3 S = 2.0261 \times 10^{-6}\sigma^3 S \tag{7}$$

where σ is given, as previously, in cm^{-1} and S in atomic units of $e^2a_0^2$. Substitution of Eq. (2) into (7) leads to

$$(2J' + 1)A = 0.66702\, \sigma^2 gf . \tag{8}$$

To determine the branching fractions it is necessary to measure the lifetime of the upper level in the case of emission or the lifetime of the lower level in the case of absorption, as well as the relative intensities of all lines originating from the considered level. The branching fraction, *BF*, is defined in the case of emission, appropriate to experimental data of interest here, as

$$BF_{ul} = \frac{A_{ul}}{\sum_k A_{uk}} = \frac{I_{ul}}{\sum_k I_{uk}} \tag{9}$$

with u standing for the upper and l the lower levels. The lifetime, τ, is defined as the inverse of the probability

$$\tau_u = \frac{1}{\sum_k A_{uk}} . \tag{10}$$

Using Eqs. (9) and (10) one obtains

$$BF_{ul} = A_{ul} \times \tau_u . \tag{11}$$

2.2. Lifetime considerations

Engman et al. [18] and Pinnington et al. [19] have used the beam-foil technique to measure radiative lifetimes of low-lying levels of the Cr II $3d^4(^5D)4p$ configuration. Later Schade et al. [20], Pinnington et al. [14], Bergeson and Lawler [10] and Nilsson et al. [11] have extended these experimental data using the time-resolved laser-induced fluorescence method. The latter technique has been improved by the use of a frequency-doubled distributed-feedback dye laser which is directly pumped by a part of a XeCl-excimer laser beam. These data are shown in Table 1.

2.3. Oscillator strength determination

To evaluate line strengths we have recourse to Eq. (5). As in previous works devoted to oscillator strength determination (see for instance [27]), the angular coefficients of the transition matrix, obtained in pure SL coupling with the help of Racah algebra is transformed into the actual intermediate coupling pertaining to our level eigenvector amplitudes, Moreover the transition integrals

$$\int_0^\infty P_{nl}(r) r P_{n'l'}(r) dr \tag{12}$$

are treated as free parameters in the least squares fit to experimental gf values. As we proceeded previously we have first sorted out the strongest lines, not blended, and particularly those representing transitions between levels with a limited number of leading components, displayed in their entirety for the reader in Tables 2 and 3 (up to 0.005%). With the combination of time-resolved laser induced fluorescence radiative lifetime determinations and FTS branching fraction measurements, Nilsson et al. [11] have generated a complete set of *gf*-values in the wavelength range 2050–4850 Å with an uncertainty varying from 3% to 42%. From these Cr II $3d^44s$–$3d^44p$ transitions we have selected in a first stage only those depopulating low-lying $3d^44p$ levels (the highly excited levels will be considered in another paper). The comparison of 119 improved experimental [11] and calculated oscillator strengths of these selected transitions (including 94 fitted values) is presented in Table 4. In the latter, we additionally have inserted some other data found in the literature. For most transitions, the observed and calculated oscillator strength values are very consistent within the experimental accuracy. Then we have extracted semi-empirically, with a very good accuracy the transition radial integral values, reported in Table 5. In this table we have inserted also the transition radial integral value of $3d^44p$–$3d^44d$, admittedly with less good accuracy since we have rooted out only the $3d^44d$ contributions to $3d^44s$ levels. Let us point out that the obtained $\langle 3d^44s|r^1|3d^44p\rangle = 2.932(0.003)$ is very close to the predicted value reported in our previous work [9], i.e. 3.00 (0.02). In the same table, we also give the results computed by means of the pseudo-relativistic Hartree–Fock (HFR) method using the basic Cowan code [17], on the one hand, and including core-polarization (HFR+CPOL), as described in [21,22], on the other hand. As a reminder, in the latter approach, the radial dipole integrals given in Eq. (12) are replaced by

$$\int_0^\infty P_{nl}(r) r \left[1 - \frac{\alpha_d}{(r^2 + r_c^2)^{3/2}}\right] P_{n'l'}(r) dr - \frac{\alpha_d}{r_c^3}\int_0^{r_c} P_{nl}(r) r P_{n'l'}(r) dr \tag{13}$$

where α_d is the dipole polarizability of the ionic core, for which numerical values can be found in the literature (see e.g. [23]), and r_c is the cut-off radius that is arbitrarily chosen as a measure of the size of the ionic core. In practice, this parameter is usually chosen to be equal to the HFR mean value $\langle r \rangle$ for the outermost ionic core orbital. In the present work, the HFR+CPOL approach was used with a Cr IV ionic core ($\alpha_d = 1.96a_0^3$ [23]; $r_c = 1.20a_0$) in addition to the explicit consideration of the following interacting configurations: $3d^5$, $3d^44s$, $3d^45s$, $3d^46s$, $3d^44d$, $3d^45d$, $3d^46d$, $3d^34s^2$, $3d^34p^2$, $3d^34d^2$, $3d^34s4d$, $3d^34s5s$ for the even parity, and $3d^44p$, $3d^45p$, $3d^46p$, $3d^44f$, $3d^45f$, $3d^46f$, $3d^34s4p$, $3d^34s4f$, $3d^34p4d$ for the odd parity. Moreover, this HFR+CPOL model was combined with a well-established semi-empirical adjustment of the radial parameters in order to minimize the discrepancies between the calculated energy levels and the available experimental values [1–7] up to 105000 cm^{-1}. In Table 1, the radiative lifetimes obtained with this method are compared with the experimental data for the low-lying $3d^44p$ energy levels. As seen from this table a very good agreement is observed, the mean ratio $\tau_{HFR+CPOL}/\tau_{exp}$

resulting to 0.96 ± 0.04 when considering the two sets of experimental lifetime values due to Schade et al. [20] and Nilsson et al. [11].

2.4. Transition probability and branching fraction derivations

After having considered the radiative lifetimes, the oscillator strengths and transition radial integrals, we propose to close this study by computing the transition probabilities and branching fractions for all transitions depopulating the low-lying $3d^4 4p$ levels (lower than 54785 cm^{-1}) and whose $\log(gf) \geq -4$, using HFR + CPOL model and to compare them with semi-empirical data of Kurucz [24]. All these data are reported in Table 6 from which a rather fairly good agreement can be observed for transitions covering a wide wavelength range, from 2344 to 7580 Å.

3. Conclusion

We have extended our previous studies concerning oscillator strengths to another singly ionized atom: Cr II. In the whole our semi-empirical calculations agree well with experimental data within the uncertainty of measurements found in the literature. Our predictions for Cr II transition radial integral values have turned out favorably thanks to this work and now we can consider as a law what we previously consider only as general trends, seeing the large number of recognized cases: a decreasing of transition radial integral values with filling nd-shells of the same principal quantum numbers for $nd^k(n+1)s \rightarrow nd^k(n+1)p$ transitions. We will check again these values in the near future since we plan to compute the gf-values of transitions depopulating higher Cr II levels than those considered in the present work.

Acknowledgments

PQ and PP are respectively Research Director and Research Associate of the Belgian Fund for Scientific Research F.R.S.-FNRS. Financial support from this organization is deeply acknowledged.

References

[1] J. Sugar, C. Corliss, J. Phys. Chem. Ref. Data Suppl. 14 (1985) 264.
[2] C.C. Kiess, J. Res. Nat. Bur. Std. 60 (1958) 375 RP2856.
[3] S. Johansson, T. Zethson, H. Hartman, et al., Astron. Astrophys. 361 (2000) 977.
[4] C.J. Sansonetti, F. Kerber, J. Reader, M.R. Rosa, Astrophys. J. Suppl. Series 153 (2004) 555.
[5] C.J. Sansonetti, G. Nave, J. Reader, F. Kerber, Astrophys. J Suppl. Series 202 (2012) 15.
[6] C.J. Sansonetti, G. Nave, Astrophys. J. Suppl. Series 213 (2014) 1.
[7] E.B. Saloman, J. Phys. Chem. Ref. Data 41 (2012) 043103.
[8] S. Bouazza, P. Quinet, P. Palmeri, (ADNDT), accepted, http://dx.doi.org/10.1016/j.adt.201705003.
[9] S. Bouazza, P. Quinet, P. Palmeri, J. Quant. Spectrosc. Radiat. Transf. 199 (2017) 66.
[10] S.D. Bergeson, J.E. Lawler, Astrophys. J. 408 (1993) 382.
[11] H. Nilsson, G. Lyung, H. Lundberg, K.E. Nielsen, Astron. Astrophys. 445 (2006) 1165.
[12] J. Musielok, T. Wujec, Astron. Astrophys. Suppl. Series 38 (1979) 119.
[13] J. Gurell, H. Nilsson, L. Engström, H. Lundberg, R. Blackwell-Whitehead, K.E. Nielsen, S. Mannervik, Astron. Astrophys. 511 (2010) A68.
[14] E.H. Pinnington, Q. Ji, B. Gou, et al., Can. J. Phys. 71 (1993) 470.
[15] I. Sobelman, Atomic Spectra and Radiative Transitions, Springer-Verlag, Berlin, 1978.
[16] J. Ruczkowski, M. Elantkowska, J. Dembczynski, J. Quant. Spectrosc. Radiat. Transf. 145 (2014) 20.
[17] R.D. Cowan, The Theory of Atomic Structure Spectra, University of California Press, Berkeley, CA, 1981.
[18] B. Engman, A. Gaupp, L.J. Curtis, I. Martinson, Phys. Scr. 12 (1975) 220.
[19] E.H. Pinnington, H.O. Lutz, G.W. Carriaveao, Nucl. Instrum. Methods 110 (1973) 55.
[20] W. Schade, B. Mundt, V. Helbig, Phys. Rev. A 42 (1990) 3.
[21] P. Quinet, P. Palmeri, E. Biémont, M.M. McCurdy, G. Rieger, E.H. Pinnington, M.E. Wickliffe, J.E. Lawler, Mon. Not. R. Astron. Soc. 307 (1999) 934.
[22] P. Quinet, P. Palmeri, E. Biémont, Z.S. Li, Z.G. Zhang, S. Svanberg, J. Alloys Compd. 344 (2002) 255.
[23] S. Fraga, J. Karwowski, K.M.S. Saxena, Handbook of Atomic Data, Elsevier Scientific Publishing Company, Amsterdam, 1976.
[24] R.L. Kurucz (1995), Atomic spectral line data from CD-ROM Nr. 23, http://www.cfa.harvard.edu/amp/ampdata/kurucz23/sekur.html.
[25] R. Spreger, B. Schelm, M. Kock, T. Neger, M. Ulbel, J. Quant. Spectrosc. Radiat. Transf. 51 (1994) 779.
[26] A.M. Gonzalez, M. Ortiz, J. Compos, Can. J. Phys. 72 (1994) 57.
[27] J. Ruczkowski, S. Bouazza, M. Elantkowska, J. Dembczynski, J. Quant. Spectrosc. Radiat. Transf. 155 (2015) 1.

Explanation of Tables

Table 1. **Comparison between HFR+CPOL radiative lifetimes (in ns) and available experimental data for low-lying $3d^4 4p$ energy levels of Cr II.**

Level: Designation of the state in LSJ coupling within the configuration and where *J* represents the total angular momentum.
Energy: Observed (experimental) energy level value in cm^{-1}.
*HFR+CPOL: Computed lifetime (in ns) using Hartree–Fock method with relativistic corrections (HFR) implemented in the code developed by Cowan [17] and including core polarization (CPOL).
Experiment: Measured lifetimes (ns) obtained by beam-foil spectroscopy or laser induced fluorescence techniques.

Table 2. **Eigenvalue components of even-parity Cr II levels of interest in this study.**

Level: Configuration to which belongs the even-parity level involved in the studied transitions and the designation of this level in LS coupling.
J: Total angular momentum.
Energy: Experimental energy level (cm^{-1}).
$3d^5$: Contribution in LS coupling of $3d^5$ configuration (in %) to the total composition of the level.
$3d^4 4s$: Contribution in LS coupling of $3d^4 4s$ configuration (in %) to the total composition of the level.
$3d^4 4d$: Contribution in LS coupling of $3d^4 4d$ configuration (in %) to the total composition of the level.
$3d^4 5s$: Contribution in LS coupling of $3d^4 5s$ configuration (in %) to the total composition of the level.
$3d^4 6s$: Contribution in LS coupling of $3d^4 6s$ configuration (in %) to the total composition of the level.
$3d^4 5d$: Contribution in LS coupling of $3d^4 5d$ configuration (in %) to the total composition of the level.
$3d^4 6d$: Contribution in LS coupling of $3d^4 6d$ configuration (in %) to the total composition of the level.
$3d^3 4s^2$: Contribution in LS coupling of $3d^3 4s^2$ configuration (in %) to the total composition of the level.

Table 3. **Eigenvalue components of odd-parity Cr II levels of interest in this study.**

Level: Configuration to which belongs the odd-parity level involved in the studied transitions and the designation of this level in LS coupling.
J: Total angular momentum.
Energy: Experimental energy level (cm^{-1}).
$3d^4 4p$: Contribution in LS coupling of $3d^4 4p$ configuration (in %) to the total composition of the level.
$3d^3 4s4p$: Contribution in LS coupling of $3d^3 4s4p$ configuration (in %) to the total composition of the level.
$3d^4 5p$: Contribution in LS coupling of $3d^4 5p$ configuration (in %) to the total composition of the level.
$3d^4 6p$: Contribution in LS coupling of $3d^4 6p$ configuration (in %) to the total composition of the level.

Table 4. **Comparison between experimental and calculated oscillator strength values.**

λ_{air}: Wavelength in air of the spectral line (Å) deduced from observed energy levels taken from [11].
Upper Level: Depopulated upper level [11] (cm^{-1}) in emission transition.
J(U): Total angular momentum of the upper level.
Lower Level: Populated lower level [11] (cm^{-1}) in emission transition.
J(L): Total angular momentum of the lower level.
gf(exp): Measured weighted oscillator strength value taken from [11] (dimensionless).
Δgf(exp): Experimental uncertainty (%) for measured weighted oscillator strength value from [11].
gf(calc): OSP weighted oscillator strength obtained in this work with help of least squares fitting procedure to experimental *gf* [11] (dimensionless). Here OSP means (oscillator strength parameterisation)
log(*gf*): Weighted oscillator strength in logarithmic scale from this work (OSP) and other studies [10–12,24–26].

Table 5. **Transition radial integral values in Cr II.**

Transition: Spectral line linking levels of mentioned configurations.
HFR: Relativistic Hartree–Fock method.
HFR+CPOL: Relativistic Hartree–Fock method including core-polarization.
OSP: Oscillator Strength Parameterization method.

Table 6. **Semi-empirical radiative data in Cr II.**

Wavelength: Wavelength in Å of experimentally observed spectral lines.
E(Lower): Energy in cm^{-1} of lower level of the transition.
Parity (Lower): Parity of lower level of the transition. ‘e’ and ‘o’ stand respectively for even and odd.
J(Lower): Total angular momentum of the lower level of the transition.
E(Upper): Energy in cm^{-1} of upper level of the transition.
Parity (Upper): Parity of upper level of the transition. ‘e’ and ‘o’ stand respectively for even and odd.
J(Upper): Total angular momentum of the upper level of the transition.
log(*gf*)(HFR+CPOL): HFR+CPOL weighted oscillator strength in logarithmic scale.
log(*gf*)(Kurucz): Weighted oscillator strength in the logarithmic scale from the Kurucz database [24].
gA(HFR+CPOL): HFR+CPOL weighted transition probability (s^{-1}).
BF (HFR+CPOL): HFR+CPOL branching fraction.

Table 1
Comparison between HFR+CPOL radiative lifetimes (in ns) and available experimental data for low-lying $3d^44p$ energy levels of Cr II.

Level	Energy	HFR+CPOL	Experiment				
	(cm^{-1})		Ref. [11]	Ref. [20]	Refs. [14,19]	Ref. [10]	Ref. [18]
$^6F_{1/2}$	46824	4.2		4.3(1)			
$^6F_{3/2}$	46906	4.1		4.2(1)			
$^6F_{5/2}$	47041	4.1		4.2(1)			
$^6F_{7/2}$	47228	4.1		4.1(1)			
$^6F_{9/2}$	47465	4.1		4.2(1)			
$^6F_{11/2}$	47752	4.0		4.0(1)			
$^6P_{3/2}$	48399	2.2		2.4(1)			
$^6P_{5/2}$	48491	2.2	2.3(2)	2.5(1)	2.45	2.4(2)	3.2(4)
$^6P_{7/2}$	48632	2.2	2.4(2)	2.5(1)	2.40(13)	2.4(2)	3.3(4)
$^4P_{1/2}$	48750	4.8		5.0(2)			
$^4P_{3/2}$	49006	4.7		4.7(2)			
$^4P_{5/2}$	49352	4.3		4.6(2)			
$^6D_{1/2}$	49493	3.8		4.3(2)			
$^6D_{3/2}$	49565	3.9		4.2(1)			
$^6D_{7/2}$	49646	3.6		3.8(1)			
$^6D_{5/2}$	49706	4.1		4.5(1)			
$^6D_{9/2}$	49838	3.6		3.8(2)			
$^4F_{3/2}$	51584	4.2	4.2(4)				
$^4F_{5/2}$	51669	4.2	4.1(4)				
$^4F_{7/2}$	51789	4.2	4.1(3)				
$^4F_{9/2}$	51943	4.2	4.1(3)				
$^4D_{1/2}$	54418	4.1	4.3(4)				
$^4D_{3/2}$	54500	4.1	4.3(4)				
$^4D_{5/2}$	54626	4.1	4.3(4)				
$^4D_{5/2}$	54784	4.1	4.3(4)		4.20(18)		

Table 2
Eigenvalue components of even-parity Cr II levels of interest in this study.

Level	*J*	Energy (cm^{-1})	$3d^5$ (%)	$3d^44s$ (%)	$3d^44d$ (%)	$3d^45s$ (%)	$3d^46s$ (%)	$3d^45d$ (%)	$3d^46d$ (%)	$3d^34s^2$ (%)
$3d^44s$ a^{6}D	1/2	11962		99.93	0.02	0.03				
$3d^44s$ a^{4}D	1/2	19528	4.36	95.35	0.16	0.02	0.03	0.01		
$3d^5$ a^{4}P	1/2	21824	97.21	1.39	0.69	0.02		0.17	0.06	0.43
$3d^44s$ a^{6}D	3/2	12033		99.93	0.02	0.03				
$3d^44s$ a^{4}D	3/2	19631	4.36	95.08	0.16	0.06	0.02	0.03	0.01	
$3d^5$ a^{4}P	3/2	21824	97.21	1.43	0.69	0.02		0.17	0.06	0.42
$3d^5$ a^{6}S	5/2	0	99.91		0.01			0.06	0.01	
$3d^44s$ a^{6}D	5/2	12148		99.93	0.02	0.03				
$3d^44s$ a^{4}D	5/2	19798	4.99	94.72	0.17	0.06	0.02	0.03	0.01	
$3d^5$ a^{4}G	5/2	20512	98.99	0.40	0.39	0.01		0.16	0.05	
$3d^5$ a^{4}P	5/2	21823	97.26	1.39	0.69	0.02		0.17		0.42
$3d^44s$ a^{6}D	7/2	12304		99.93	0.02	0.03				
$3d^44s$ a^{4}D	7/2	20024	5.17	94.53	0.17	0.06	0.02	0.03	0.01	
$3d^5$ a^{4}G	7/2	20518	99.00	0.40	0.39	0.01		0.15	0.05	
$3d^44s$ a^{6}D	9/2	12496		99.93	0.02	0.03				
$3d^5$ a^{4}G	11/2	20512	99.02	0.38	0.38	0.01		0.15	0.05	

Table 3
Eigenvalue components of odd-parity Cr II levels of interest in this study.

Level	J	Energy (cm^{-1})	$3d^44p$ (%)	$3d^34s4p$ (%)	$3d^45p$ (%)	$3d^46p$ (%)
z^6F	1/2	46823	99.57	0.10	0.27	0.06
z^4P	1/2	48749	99.62	0.22	0.12	0.03
z^6D	1/2	49493	99.52	0.31	0.13	0.02
z^4D	1/2	54418	99.48	0.37	0.11	0.03
z^6F	3/2	46905	99.57	0.10	0.27	0.06
z^6P	3/2	48399	99.74	0.13	0.09	0.03
z^4P	3/2	49006	99.62	0.23	0.12	0.03
z^6D	3/2	49565	99.52	0.31	0.13	0.02
z^4D	3/2	54499	99.49	0.37	0.11	0.03
z^6F	5/2	47040	99.57	0.10	0.27	0.06
z^6P	5/2	48391	99.74	0.13	0.09	0.03
z^6D	5/2	49352	99.59	0.26	0.13	0.03
z^4P	5/2	49706	99.56	0.28	0.13	0.02
z^6F	7/2	47227	99.57	0.10	0.27	0.06
z^6P	7/2	48632	99.74	0.13	0.09	0.03
z^6D	7/2	49646	99.49	0.35	0.14	0.02
z^4F	7/2	51789	99.74	0.14	0.09	0.02
z^4D	7/2	54784	99.49	0.36	0.11	0.03
z^6F	9/2	47465	99.57	0.10	0.27	0.06
z^6D	9/2	49838	99.49	0.34	0.14	0.02
z^4F	9/2	51943	99.74	0.14	0.09	0.02

Table 4
Comparison between experimental and calculated oscillator strength values.

λ_{air}	Upper Level	J(U)	Lower Level	J(L)	gf(exp)	Δgf(exp)	gf(calc)	log(gf)						
(Å)	(cm^{-1})		(cm^{-1})			(%)		[11]	OSP	[24]	[25]	[10]	[26]	[12]
2531.85	51788.816	7/2	12303.82	7/2	0.0182	12	0.0106	−1.740	−1.9756	−1.878				
2534.33	51942.664	9/2	12496.456	9/2	0.0484	12	0.0345	−1.315	−1.4616	−1.361				
2653.58	49706.262	5/2	12032.545	3/2	0.2415	6	0.4034	−0.617	−0.3943	−0.304				
2658.59	49564.504	3/2	11961.747	1/2	0.2642	8	0.3447	−0.578	−0.4626	−0.45				
2661.72	49706.262	5/2	12147.772	5/2	0.0728	6	0.1355	−1.138	−0.8681	−0.755				
2663.42	49838.379	9/2	12303.82	7/2	0.561	40	0.633	−0.251	−0.1986	−0.205				
2663.60	49564.504	3/2	12032.545	3/2	0.0238	9	0.0049	−1.623	−2.3056	−2.181				
2663.67	49492.711	1/2	11961.747	1/2	0.0912	8	0.1127	−1.040	−0.9480	−0.973				
2666.01	49645.805	7/2	12147.772	5/2	0.7834	23	0.8761	−0.106	−0.0574	−0.064	−0.1		−0.056	−0.313
2668.71	49492.711	1/2	12032.545	3/2	0.3097	8	0.3863	−0.509	−0.4131	−0.448	−0.67		−0.537	−0.557
2671.81	49564.504	3/2	12147.772	5/2	0.4667	7	0.5881	−0.331	−0.2306	−0.271	−0.34		−0.373	−0.377
2672.83	49706.262	5/2	12303.82	7/2	0.369	6	0.5366	−0.433	−0.2703	−0.281	−0.59			−0.468
2678.79	49351.734	5/2	12032.545	3/2	0.5176	7	0.4382	−0.286	−0.3583	−0.475	−0.39		−0.351	
2687.09	49351.734	5/2	12147.772	5/2	0.2786	7	0.2565	−0.555	−0.5908	−0.674	−0.6		−0.608	
2691.04	49645.805	7/2	12496.456	9/2	0.4446	23	0.5079	−0.352	−0.2942	−0.403			−0.337	
2698.41	49351.734	5/2	12303.82	7/2	0.2871	8	0.1931	−0.542	−0.7143	−1.077				
2698.68	49005.848	3/2	11961.747	1/2	0.2729	6	0.2362	−0.564	−0.6268	−0.656				
2703.85	49005.848	3/2	12032.545	3/2	0.0406	7	0.043	−1.392	−1.3664	−1.327				
2712.31	49005.848	3/2	12147.772	5/2	0.159	6	0.106	−0.799	−0.9746	−1.167	−0.76			
2717.51	48749.277	1/2	11961.747	1/2	0.0372	8	0.0308	−1.430	−1.5121	−1.543				
2722.75	48749.277	1/2	12032.545	3/2	0.1361	6	0.1077	−0.866	−0.9678	−1.014	−1.002			
2740.10	48632.059	7/2	12147.772	5/2	0.0798	12	0.081	−1.098	−1.0917	−1.233	−1.18	−1.09	−1.091	−1.004
2742.03	48491.059	5/2	12032.545	3/2	0.2042	9	0.1945	−0.690	−0.7111	−0.817	−0.82	−0.68	−0.626	
2743.64	48398.871	3/2	11961.747	1/2	0.3459	9	0.3349	−0.461	−0.4751	−0.545		−0.47	−0.47	
2748.98	48398.871	3/2	12032.545	3/2	0.527	9	0.5378	−0.278	−0.2694	−0.305	−0.52	−0.28	−0.257	
2750.73	48491.059	5/2	12147.772	5/2	0.6501	9	0.6714	−0.187	−0.1730	−0.226	−0.43	−0.18	−0.199	
2751.86	48632.059	7/2	12303.82	7/2	0.5058	9	0.5286	−0.296	−0.2769	−0.349	−0.69	−0.29	−0.294	
2757.73	48398.871	3/2	12147.772	5/2	0.455	9	0.4463	−0.342	−0.3504	−0.349	−0.53	−0.36	−0.372	
2762.59	48491.059	5/2	12303.82	7/2	1.0914	9	1.1292	0.038	0.0528	0.048	−0.28	0.05	0.024	
2766.53	48632.059	7/2	12496.456	9/2	2.0512	9	2.1053	0.312	0.3233	0.31		0.32	0.301	
2835.63	47751.602	11/2	12496.456	9/2	3.6141	3	3.8391	0.558	0.5842	0.572			0.562	
2849.83	47227.219	7/2	12147.772	5/2	1.4852	3	1.6041	0.171	0.2052	0.184	0.13		0.15	−0.067
2855.67	47040.273	5/2	12032.545	3/2	0.8299	4	0.8964	−0.081	−0.0475	−0.069	−0.18		−0.101	
2856.76	54625.594	5/2	19631.205	3/2	0.241	10	0.3301	−0.618	−0.4813	−0.598	−0.71		−0.511	
2857.40	54784.449	7/2	19797.859	5/2	0.2061	11	0.2549	−0.686	−0.5937	−0.698			−0.562	
2858.65	54499.492	3/2	19528.23	1/2	0.1832	11	0.25	−0.737	−0.6021	−0.726				
2858.91	47464.559	9/2	12496.456	9/2	0.597	6	0.6208	−0.224	−0.2071	−0.196			−0.179	
2860.93	46905.137	3/2	11961.747	1/2	0.3556	5	0.3882	−0.449	−0.4110	−0.432			−0.503	−0.49
2862.57	47227.219	7/2	12303.82	7/2	0.8511	5	0.8844	−0.070	−0.0534	−0.053	−0.45	−0.034	−0.229	
2865.10	47040.273	5/2	12147.772	5/2	0.8166	4	0.8906	−0.088	−0.0503	−0.057	−0.12		−0.045	
2865.33	54417.957	1/2	19528.23	1/2	0.1901	11	0.2799	−0.721	−0.5530	−0.688				
2867.09	54499.492	3/2	19631.205	3/2	0.3251	10	0.4636	−0.488	−0.3339	−0.474				−0.266
2867.65	46823.305	1/2	11961.747	1/2	0.4365	3	0.4902	−0.360	−0.3096	−0.324			−0.353	−0.567
2873.48	46823.305	1/2	12032.545	3/2	0.138	6	0.1417	−0.860	−0.8486	−0.853			−0.843	
2873.81	54417.957	1/2	19631.205	3/2	0.2104	11	0.2965	−0.677	−0.5279	−0.662				−0.672
2875.99	54784.449	7/2	20024.012	7/2	1.531	10	2.0221	0.185	0.3058	0.175				
2876.24	46905.137	3/2	12147.772	5/2	0.1462	5	0.155	−0.835	−0.8096	−0.804			−0.58	
2878.44	47227.219	7/2	12496.456	9/2	0.0481	8	0.0499	−1.318	−1.3016	−1.27			−1.304	−1.158
2880.86	54499.492	3/2	19797.859	5/2	0.317	10	0.4369	−0.499	−0.3596	−0.493				−0.411
2889.19	54625.594	5/2	20024.012	7/2	0.278	10	0.3752	−0.556	−0.4258	−0.554				
3032.92	54784.449	7/2	21822.506	5/2	0.0486	20	0.0959	−1.313	−1.0183	−1.031				
3047.61	54625.594	5/2	21824.141	3/2	0.0263	21	0.0535	−1.580	−1.2717	−1.326				
3118.65	51584.102	3/2	19528.23	1/2	0.7907	10	0.6897	−0.102	−0.1613	−0.081				−0.004

(*continued on next page*)

Table 4 (*continued*)

λ_{air}	Upper Level	J(U)	Lower Level	J(L)	gf(exp)	Δgf(exp)	gf(calc)	log(gf)						
(Å)	(cm^{-1})		(cm^{-1})			(%)		[11]	OSP	[24]	[25]	[10]	[26]	[12]
3124.98	51788.816	7/2	19797.859	5/2	1.932	8	1.6578	0.286	0.2195	0.303	0.44			
3128.70	51584.102	3/2	19631.205	3/2	0.2965	11	0.2452	−0.528	−0.6105	−0.511	−0.82			−0.362
3132.05	51942.664	9/2	20024.012	7/2	2.7353	7	2.308	0.437	0.3632	0.451	0.57			
3136.69	51669.406	5/2	19797.859	5/2	0.3855	11	0.2978	−0.414	−0.5260	−0.416	−0.29			−0.254
3147.22	51788.816	7/2	20024.012	7/2	0.2965	9	0.2087	−0.528	−0.6805	−0.558	−0.18			
3180.69	51942.664	9/2	20512.098	11/2	0.6383	9	0.4372	−0.195	−0.3593	−0.131				
3209.18	51669.406	5/2	20517.793	7/2	0.3882	11	0.2476	−0.411	−0.6063	−0.372				−0.214
3217.40	51584.102	3/2	20512.062	5/2	0.2704	11	0.1831	−0.568	−0.7373	−0.501				−0.332
3324.06	49706.262	5/2	19631.205	3/2	0.0296	14	0.0216	−1.529	−1.6648	−1.691	−1.21			
3328.35	49564.504	3/2	19528.23	1/2	0.0196	22	0.0156	−1.708	−1.8067	−1.752				
3336.33	49492.711	1/2	19528.23	1/2	0.0673	14	0.0495	−1.172	−1.3054	−1.172				
3339.80	49564.504	3/2	19631.205	3/2	0.1057	13	0.0762	−0.976	−1.1182	−1.044	−1.03			
3342.58	49706.262	5/2	19797.859	5/2	0.1545	6	0.1081	−0.811	−0.9660	−1.03	−0.51			
3347.83	49492.711	1/2	19631.205	3/2	0.0705	14	0.046	−1.152	−1.3371	−1.17	−1.24			
3353.12	49838.379	9/2	20024.012	7/2	0.0244	42	0.0203	−1.613	−1.6918	−1.477	−0.97			
3358.50	49564.504	3/2	19797.859	5/2	0.2143	13	0.1399	−0.669	−0.8543	−0.722	−0.44			
3368.05	49706.262	5/2	20024.012	7/2	0.6839	5	0.4469	−0.165	−0.3498	−0.319	0.18			
3382.68	49351.734	5/2	19797.859	5/2	0.1052	8	0.1567	−0.978	−0.8048	−0.639	−0.7			−0.354
3391.43	49005.848	3/2	19528.23	1/2	0.04	11	0.0342	−1.398	−1.4655	−1.35				−0.906
3403.26	54417.957	1/2	25042.76	3/2	0.067	16	0.0702	−1.174	−1.1537	−1.054				−0.508
3403.32	49005.848	3/2	19631.205	3/2	0.2168	7	0.2121	−0.664	−0.6735	−0.536				
3408.77	49351.734	5/2	20024.012	7/2	0.3767	9	0.5267	−0.424	−0.2784	−0.038	−0.048			−0.017
3421.21	48749.277	1/2	19528.23	1/2	0.1905	7	0.1742	−0.720	−0.7589	−0.611				−0.224
3422.74	49005.848	3/2	19797.859	5/2	0.3776	6	0.3515	−0.423	−0.4541	−0.266	−0.15			−0.039
3433.31	48749.277	1/2	19631.205	3/2	0.1866	7	0.158	−0.729	−0.8014	−0.624				−0.338
3475.13	48398.871	3/2	19631.205	3/2	0.024	20	0.0105	−1.620	−1.9808	−1.764				
3495.38	48398.871	3/2	19797.859	5/2	0.0197	22	0.0152	−1.706	−1.8187	−1.539				
3511.83	48491.059	5/2	20024.012	7/2	0.0346	17	0.019	−1.461	−1.7205	−1.452	−1.46			−1.074
3585.30	49706.262	5/2	21822.506	5/2	0.1991	6	0.0315	−0.701	−1.5012	−1.144				
3585.50	49706.262	5/2	21824.141	3/2	0.0412	10	0.0151	−1.385	−1.8203	−1.517				
3631.47	49351.734	5/2	21822.506	5/2	0.0594	10	0.0364	−1.226	−1.4388	−0.846				
3631.68	49351.734	5/2	21824.141	3/2	0.0208	16	0.0181	−1.682	−1.7428	−1.253				
3677.68	49005.848	3/2	21822.506	5/2	0.0308	11	0.045	−1.511	−1.3470	−1.266				
3677.84	49005.848	3/2	21823.725	1/2	0.0314	11	0.0212	−1.503	−1.6737	−1.247				
3712.95	48749.277	1/2	21824.141	3/2	0.0469	9	0.0353	−1.329	−1.4521	−1.243				

Table 5
Transition radial integral values in Cr II.

Transition	HFR	HFR+CPOL	OSP
$3d^44s - 3d^44p$	3.184	2.969	2.932±0.003
$3d^5 - 3d^44p$	1.567	1.503	1.413±0.008
$3d^44d - 3d^44p$	5.097	4.944	5.11±0.09

Table 6
Semi-empirical radiative data in Cr II.

Wavelength (Å)	*E*(Lower) (cm^{-1})	Parity (Lower)	*J*(Lower)	*E*(Upper) (cm^{-1})	Parity (Upper)	*J*(Upper)	log(*gf*)(HFR+CPOL)	log(*gf*) (Kurucz)	*gA* (HFR+CPOL) (s^{-1})	*BF* (HFR+CPOL)
1825.335	0	(e)	2.5	54784	(o)	3.5	−3.28	−2.944	1.07E+06	5.75E−04
1830.644	0	(e)	2.5	54626	(o)	2.5	−3.93	−3.602	2.38E+05	1.71E−04
2011.169	0	(e)	2.5	49706	(o)	2.5	−2.73	−3.960	3.14E+06	2.36E−03
2016.922	0	(e)	2.5	49565	(o)	1.5	−3.33	−4.848	7.79E+05	8.18E−04
2025.619	0	(e)	2.5	49352	(o)	2.5	−2.42	−1.549	6.20E+06	4.75E−03
2039.918	0	(e)	2.5	49006	(o)	1.5	−2.43	−1.577	6.05E+06	7.11E−03
2055.599	0	(e)	2.5	48632	(o)	3.5	−0.03	0.025	1.48E+09	4.44E−01
2061.577	0	(e)	2.5	48491	(o)	2.5	−0.16	−0.114	1.09E+09	4.18E−01
2065.504	0	(e)	2.5	48399	(o)	1.5	−0.34	−0.297	7.20E+08	4.32E−01
2344.680	12148	(e)	2.5	54784	(o)	3.5	−3.85	−3.463	1.72E+05	9.25E−05
2347.082	12033	(e)	1.5	54626	(o)	2.5	−3.65	−3.296	2.70E+05	1.94E−04
2350.134	11962	(e)	0.5	54499	(o)	1.5	−3.74	−3.430	2.19E+05	2.35E−04
2353.449	12148	(e)	2.5	54626	(o)	2.5	−3.12	−2.985	9.20E+05	6.59E−04
2354.052	12033	(e)	1.5	54499	(o)	1.5	−3.22	−3.044	7.25E+05	7.79E−04
2354.648	11962	(e)	0.5	54418	(o)	0.5	−3.41	−3.203	4.67E+05	1.00E−03
2362.128	12304	(e)	3.5	54626	(o)	2.5	−3.76	−3.274	2.10E+05	1.51E−04
2521.879	12148	(e)	2.5	51789	(o)	3.5	−3.43	−4.800	3.85E+05	1.97E−04
2527.585	12033	(e)	1.5	51584	(o)	1.5	−3.54	−3.240	3.00E+05	3.15E−04
2529.499	12148	(e)	2.5	51669	(o)	2.5	−2.68	−2.477	2.17E+06	1.48E−03
2534.971	12148	(e)	2.5	51584	(o)	1.5	−3.43	−3.329	3.81E+05	4.00E−04
2539.527	12304	(e)	3.5	51669	(o)	2.5	−2.82	−2.764	1.56E+06	1.07E−03
2653.581	12033	(e)	1.5	49706	(o)	2.5	−0.46	−0.650	3.28E+08	2.46E−01
2658.588	11962	(e)	0.5	49565	(o)	1.5	−0.50	−0.610	2.98E+08	3.13E−01
2661.722	12148	(e)	2.5	49706	(o)	2.5	−0.91	−0.755	1.16E+08	8.70E−02
2663.604	12033	(e)	1.5	49565	(o)	1.5	−2.29	−2.181	4.87E+06	5.11E−03
2663.674	11962	(e)	0.5	49493	(o)	0.5	−0.98	−0.973	9.80E+07	2.11E−01
2666.014	12148	(e)	2.5	49646	(o)	3.5	−0.12	−0.300	7.23E+08	3.43E−01
2668.709	12033	(e)	1.5	49493	(o)	0.5	−0.44	−0.520	3.40E+08	7.31E−01
2671.807	12148	(e)	2.5	49565	(o)	1.5	−0.26	−0.370	5.15E+08	5.41E−01
2672.828	12304	(e)	3.5	49706	(o)	2.5	−0.33	−0.450	4.42E+08	3.32E−01
2678.791	12033	(e)	1.5	49352	(o)	2.5	−0.43	−0.475	3.50E+08	2.68E−01
2687.088	12148	(e)	2.5	49352	(o)	2.5	−0.71	−0.674	1.82E+08	1.40E−01
2698.407	12304	(e)	3.5	49352	(o)	2.5	−0.58	−1.077	2.45E+08	1.88E−01
2698.684	11962	(e)	0.5	49006	(o)	1.5	−0.79	−0.656	1.48E+08	1.74E−01
2703.852	12033	(e)	1.5	49006	(o)	1.5	−1.78	−1.327	1.53E+07	1.80E−02
2712.306	12148	(e)	2.5	49006	(o)	1.5	−0.86	−1.167	1.26E+08	1.48E−01
2717.507	11962	(e)	0.5	48749	(o)	0.5	−1.58	−1.543	2.40E+07	6.00E−02
2722.747	12033	(e)	1.5	48749	(o)	0.5	−1.02	−1.014	8.54E+07	2.14E−01
2740.095	12148	(e)	2.5	48632	(o)	3.5	−1.05	−1.000	7.87E+07	2.36E−02
2742.032	12033	(e)	1.5	48491	(o)	2.5	−0.67	−0.817	1.88E+08	7.21E−02
2743.642	11962	(e)	0.5	48399	(o)	1.5	−0.45	−0.545	3.12E+08	1.87E−01
2748.984	12033	(e)	1.5	48399	(o)	1.5	−0.29	−0.305	4.47E+08	2.68E−01
2750.727	12148	(e)	2.5	48491	(o)	2.5	−0.18	−0.226	5.78E+08	2.22E−01
2757.722	12148	(e)	2.5	48399	(o)	1.5	−0.44	−0.349	3.14E+08	1.88E−01
2762.589	12304	(e)	3.5	48491	(o)	2.5	−0.02	0.048	8.36E+08	3.20E−01
2849.834	12148	(e)	2.5	47227	(o)	3.5	0.18	−0.050	1.26E+09	6.46E−01
2855.673	12033	(e)	1.5	47040	(o)	2.5	−0.07	−0.069	7.01E+08	4.91E−01
2856.762	19631	(e)	1.5	54626	(o)	2.5	−0.65	−0.500	1.82E+08	1.30E−01
2857.398	19798	(e)	2.5	54784	(o)	3.5	−0.75	−0.560	1.47E+08	7.90E−02
2858.651	19528	(e)	0.5	54499	(o)	1.5	−0.79	−0.726	1.34E+08	1.44E−01
2860.931	11962	(e)	0.5	46905	(o)	1.5	−0.43	−0.470	3.02E+08	3.17E−01
2865.104	12148	(e)	2.5	47040	(o)	2.5	−0.08	−0.057	6.71E+08	4.70E−01
2865.332	19528	(e)	0.5	54418	(o)	0.5	−0.76	−0.688	1.42E+08	3.05E−01

(continued on next page)

Table 6 *(continued)*

Wavelength (Å)	E(Lower) (cm^{-1})	Parity (Lower)	J(Lower)	E(Upper) (cm^{-1})	Parity (Upper)	J(Upper)	log(gf)(HFR+CPOL)	log(gf) (Kurucz)	gA (HFR+CPOL) (s^{-1})	BF (HFR+CPOL)
2866.740	12033	(e)	1.5	46905	(o)	1.5	−0.17	−0.230	5.49E+08	5.76E−01
2867.094	19631	(e)	1.5	54499	(o)	1.5	−0.55	−0.270	2.29E+08	2.46E−01
2867.647	11962	(e)	0.5	46823	(o)	0.5	−0.34	−0.570	3.75E+08	8.06E−01
2870.432	19798	(e)	2.5	54626	(o)	2.5	−0.21	−0.020	4.99E+08	3.58E−01
2873.483	12033	(e)	1.5	46823	(o)	0.5	−0.88	−0.853	1.06E+08	2.28E−01
2873.814	19631	(e)	1.5	54418	(o)	0.5	−0.73	−0.660	1.50E+08	3.23E−01
2876.244	12148	(e)	2.5	46905	(o)	1.5	−0.85	−0.804	1.14E+08	1.20E−01
2877.975	12304	(e)	3.5	47040	(o)	2.5	−1.00	−0.931	8.11E+07	5.68E−02
2880.864	19798	(e)	2.5	54499	(o)	1.5	−0.57	−0.410	2.18E+08	2.34E−01
2889.194	20024	(e)	3.5	54626	(o)	2.5	−0.63	−0.554	1.88E+08	1.35E−01
3032.919	21823	(e)	2.5	54784	(o)	3.5	−1.12	−1.031	5.46E+07	2.93E−02
3047.607	21823	(e)	2.5	54626	(o)	2.5	−1.21	−1.234	4.41E+07	3.16E−02
3047.759	21824	(e)	1.5	54626	(o)	2.5	−1.43	−1.326	2.68E+07	1.92E−02
3059.368	21823	(e)	2.5	54499	(o)	1.5	−1.88	−1.941	9.39E+06	1.01E−02
3059.482	21824	(e)	0.5	54499	(o)	1.5	−1.76	−1.675	1.23E+07	1.32E−02
3059.521	21824	(e)	1.5	54499	(o)	1.5	−1.30	−1.287	3.58E+07	3.85E−02
3067.136	21824	(e)	0.5	54418	(o)	0.5	−1.51	−1.473	2.20E+07	4.73E−02
3067.175	21824	(e)	1.5	54418	(o)	0.5	−1.91	−1.927	8.77E+06	1.89E−02
3118.649	19528	(e)	0.5	51584	(o)	1.5	−0.11	0.000	5.25E+08	5.51E−01
3120.369	19631	(e)	1.5	51669	(o)	2.5	0.09	0.120	8.39E+08	5.73E−01
3124.977	19798	(e)	2.5	51789	(o)	3.5	0.27	−0.018	1.26E+09	6.46E−01
3128.700	19631	(e)	1.5	51584	(o)	1.5	−0.54	−0.320	1.96E+08	2.06E−01
3136.686	19798	(e)	2.5	51669	(o)	2.5	−0.44	−0.250	2.44E+08	1.67E−01
3145.104	19798	(e)	2.5	51584	(o)	1.5	−1.75	−1.733	1.20E+07	1.26E−02
3159.103	20024	(e)	3.5	51669	(o)	2.5	−1.94	−1.950	7.58E+06	5.18E−03
3196.339	20512	(e)	2.5	51789	(o)	3.5	−2.88	−2.827	8.44E+05	4.33E−04
3208.589	20512	(e)	2.5	51669	(o)	2.5	−1.33	−1.307	3.03E+07	2.07E−02
3209.179	20518	(e)	3.5	51669	(o)	2.5	−0.40	−0.200	2.58E+08	1.76E−01
3217.398	20512	(e)	2.5	51584	(o)	1.5	−0.52	−0.320	1.91E+08	2.01E−01
3324.058	19631	(e)	1.5	49706	(o)	2.5	−1.60	−1.691	1.53E+07	1.15E−02
3328.350	19528	(e)	0.5	49565	(o)	1.5	−1.72	−1.752	1.15E+07	1.21E−02
3336.121	21823	(e)	2.5	51789	(o)	3.5	−2.15	−2.695	4.20E+06	2.15E−03
3336.325	19528	(e)	0.5	49493	(o)	0.5	−1.19	−0.850	3.89E+07	8.36E−02
3339.801	19631	(e)	1.5	49565	(o)	1.5	−1.01	−0.480	5.82E+07	6.11E−02
3342.581	19798	(e)	2.5	49706	(o)	2.5	−0.87	−0.410	8.00E+07	6.00E−02
3347.831	19631	(e)	1.5	49493	(o)	0.5	−1.19	−0.760	3.87E+07	8.32E−02
3349.351	19798	(e)	2.5	49646	(o)	3.5	−2.16	−2.128	4.15E+06	1.97E−03
3349.469	21823	(e)	2.5	51669	(o)	2.5	−2.91	−3.520	7.29E+05	4.98E−04
3349.652	21824	(e)	1.5	51669	(o)	2.5	−2.55	−3.123	1.66E+06	1.13E−03
3358.500	19798	(e)	2.5	49565	(o)	1.5	−0.69	−0.130	1.20E+08	1.26E−01
3359.207	21824	(e)	0.5	51584	(o)	1.5	−3.32	−4.773	2.79E+05	2.93E−04
3359.254	21824	(e)	1.5	51584	(o)	1.5	−3.21	−3.925	3.56E+05	3.74E−04
3361.765	25047	(e)	2.5	54784	(o)	3.5	−0.84	−0.926	8.48E+07	4.56E−02
3363.711	19631	(e)	1.5	49352	(o)	2.5	−1.88	−1.695	7.88E+06	6.04E−03
3368.049	20024	(e)	3.5	49706	(o)	2.5	−0.18	0.150	3.93E+08	2.95E−01
3378.330	25034	(e)	3.5	54626	(o)	2.5	−0.81	−0.380	9.06E+07	6.49E−02
3379.368	25043	(e)	1.5	54626	(o)	2.5	−0.79	−0.310	9.57E+07	6.86E−02
3379.820	25047	(e)	2.5	54626	(o)	2.5	−0.43	−0.548	2.18E+08	1.56E−01
3382.680	19798	(e)	2.5	49352	(o)	2.5	−0.75	−0.330	1.04E+08	7.97E−02
3391.431	19528	(e)	0.5	49006	(o)	1.5	−1.37	−0.880	2.49E+07	2.93E−02
3392.981	25035	(e)	0.5	54499	(o)	1.5	−0.95	−0.500	6.49E+07	6.98E−02
3393.836	25043	(e)	1.5	54499	(o)	1.5	−0.78	−0.340	9.61E+07	1.03E−01
3394.291	25047	(e)	2.5	54499	(o)	1.5	−0.77	−0.290	9.90E+07	1.06E−01
3402.397	25035	(e)	0.5	54418	(o)	0.5	−0.97	−0.560	6.14E+07	1.32E−01

(*continued on next page*)

Table 6 (*continued*)

Wavelength (Å)	*E*(Lower) (cm^{-1})	Parity (Lower)	*J*(Lower)	*E*(Upper) (cm^{-1})	Parity (Upper)	*J*(Upper)	log(*gf*)(HFR+CPOL)	log(*gf*) (Kurucz)	*gA* (HFR+CPOL) (s^{-1})	*BF* (HFR+CPOL)
3403.256	25043	(e)	1.5	54418	(o)	0.5	−0.94	−1.054	6.60E+07	1.42E−01
3403.320	19631	(e)	1.5	49006	(o)	1.5	−0.54	−0.536	1.65E+08	1.94E−01
3408.765	20024	(e)	3.5	49352	(o)	2.5	−0.14	0.000	4.18E+08	3.20E−01
3421.209	19528	(e)	0.5	48749	(o)	0.5	−0.62	−0.220	1.39E+08	3.48E−01
3422.739	19798	(e)	2.5	49006	(o)	1.5	−0.26	−0.010	3.12E+08	3.67E−01
3425.028	20518	(e)	3.5	49706	(o)	2.5	−3.79	−3.520	9.13E+04	6.85E−05
3433.309	19631	(e)	1.5	48749	(o)	0.5	−0.62	−0.340	1.36E+08	3.40E−01
3462.734	19528	(e)	0.5	48399	(o)	1.5	−3.15	−2.541	3.87E+05	2.32E−04
3464.029	19631	(e)	1.5	48491	(o)	2.5	−3.19	−2.769	3.54E+05	1.36E−04
3467.111	19798	(e)	2.5	48632	(o)	3.5	−3.72	−3.655	1.04E+05	3.12E−05
3467.142	20518	(e)	3.5	49352	(o)	2.5	−3.54	−3.791	1.60E+05	1.23E−04
3475.130	19631	(e)	1.5	48399	(o)	1.5	−2.39	−1.764	2.20E+06	1.32E−03
3484.149	19798	(e)	2.5	48491	(o)	2.5	−2.40	−1.903	2.16E+06	8.28E−04
3495.379	19798	(e)	2.5	48399	(o)	1.5	−2.17	−1.824	3.65E+06	2.19E−03
3511.829	20024	(e)	3.5	48491	(o)	2.5	−1.95	−1.060	5.99E+06	2.30E−03
3585.294	21823	(e)	2.5	49706	(o)	2.5	−0.97	−1.144	5.57E+07	4.18E−02
3585.504	21824	(e)	1.5	49706	(o)	2.5	−1.36	−1.517	2.26E+07	1.70E−02
3603.615	21823	(e)	2.5	49565	(o)	1.5	−1.79	−1.722	8.36E+06	8.78E−03
3603.773	21824	(e)	0.5	49565	(o)	1.5	−1.66	−1.693	1.13E+07	1.19E−02
3603.827	21824	(e)	1.5	49565	(o)	1.5	−2.04	−2.148	4.64E+06	4.87E−03
3613.124	21824	(e)	0.5	49493	(o)	0.5	−2.56	−2.480	1.40E+06	3.01E−03
3613.179	21824	(e)	1.5	49493	(o)	0.5	−1.85	−1.779	7.24E+06	1.56E−02
3631.467	21823	(e)	2.5	49352	(o)	2.5	−0.93	−0.846	6.02E+07	4.62E−02
3631.683	21824	(e)	1.5	49352	(o)	2.5	−1.35	−1.253	2.27E+07	1.74E−02
3644.690	19798	(e)	2.5	47227	(o)	3.5	−2.74	−2.379	9.08E+05	4.65E−04
3647.388	19631	(e)	1.5	47040	(o)	2.5	−2.92	−2.600	5.98E+05	4.19E−04
3651.673	19528	(e)	0.5	46905	(o)	1.5	−3.28	−2.993	2.63E+05	2.76E−04
3662.621	19528	(e)	0.5	46823	(o)	0.5	−3.95	−3.788	5.55E+04	1.19E−04
3677.676	21823	(e)	2.5	49006	(o)	1.5	−1.38	−1.420	2.07E+07	2.43E−02
3677.841	21824	(e)	0.5	49006	(o)	1.5	−1.25	−1.390	2.79E+07	3.28E−02
3677.898	21824	(e)	1.5	49006	(o)	1.5	−1.61	−1.854	1.22E+07	1.43E−02
3712.887	21824	(e)	0.5	48749	(o)	0.5	−2.03	−1.961	4.48E+06	1.12E−02
3712.945	21824	(e)	1.5	48749	(o)	0.5	−1.31	−1.201	2.37E+07	5.93E−02
3738.359	25047	(e)	2.5	51789	(o)	3.5	−1.25	−1.975	2.66E+07	1.36E−02
3748.669	21823	(e)	2.5	48491	(o)	2.5	−2.59	−2.194	1.19E+06	4.56E−04
3748.899	21824	(e)	1.5	48491	(o)	2.5	−3.16	−2.680	3.25E+05	1.25E−04
3754.569	25043	(e)	1.5	51669	(o)	2.5	−1.46	−2.188	1.61E+07	1.10E−02
3755.127	25047	(e)	2.5	51669	(o)	2.5	−2.31	−4.233	2.27E+06	1.55E−03
3761.672	21823	(e)	2.5	48399	(o)	1.5	−3.14	−2.514	3.39E+05	2.03E−04
3761.845	21824	(e)	0.5	48399	(o)	1.5	−3.14	−2.511	3.37E+05	2.02E−04
3761.904	21824	(e)	1.5	48399	(o)	1.5	−3.45	−2.892	1.63E+05	9.78E−05
3765.585	25035	(e)	0.5	51584	(o)	1.5	−1.72	−2.499	8.88E+06	9.32E−03
3766.637	25043	(e)	1.5	51584	(o)	1.5	−2.34	−3.620	2.14E+06	2.25E−03
4054.079	25047	(e)	2.5	49706	(o)	2.5	−3.31	−2.475	1.97E+05	1.48E−04
4064.043	25047	(e)	2.5	49646	(o)	3.5	−3.53	−4.370	1.19E+05	5.65E−05
4072.556	29952	(e)	0.5	54499	(o)	1.5	−2.40	−2.407	1.60E+06	1.72E−03
4086.128	29952	(e)	0.5	54418	(o)	0.5	−2.44	−2.422	1.46E+06	3.14E−03
4110.982	30307	(e)	1.5	54626	(o)	2.5	−2.02	−2.023	3.78E+06	2.71E−03
4112.547	25043	(e)	1.5	49352	(o)	2.5	−3.66	−3.019	8.67E+04	6.65E−05
4113.216	25047	(e)	2.5	49352	(o)	2.5	−3.56	−2.274	1.09E+05	8.36E−05
4132.411	30307	(e)	1.5	54499	(o)	1.5	−2.38	−2.345	1.63E+06	1.75E−03
4146.386	30307	(e)	1.5	54418	(o)	0.5	−3.18	−3.149	2.59E+05	5.57E−04
4179.421	30864	(e)	2.5	54784	(o)	3.5	−1.77	−1.773	6.47E+06	3.48E−03

(*continued on next page*)

Table 6 (*continued*)

Wavelength (Å)	*E*(Lower) (cm^{-1})	Parity (Lower)	*J*(Lower)	*E*(Upper) (cm^{-1})	Parity (Upper)	*J*(Upper)	log(*gf*)(HFR+CPOL)	log(*gf*) (Kurucz)	*gA* (HFR+CPOL) (s^{-1})	*BF* (HFR+CPOL)
4207.363	30864	(e)	2.5	54626	(o)	2.5	−2.86	−2.475	5.29E+05	3.79E−04
4224.081	31117	(e)	2.5	54784	(o)	3.5	−3.99	−3.526	3.94E+04	2.12E−05
4229.812	30864	(e)	2.5	54499	(o)	1.5	−2.72	−3.324	7.13E+05	7.66E−04
4246.404	31083	(e)	1.5	54626	(o)	2.5	−2.99	−3.218	3.82E+05	2.74E−04
4252.625	31117	(e)	2.5	54626	(o)	2.5	−1.75	−2.018	6.69E+06	4.79E−03
4261.917	31169	(e)	3.5	54626	(o)	2.5	−1.26	−1.531	2.08E+07	1.49E−02
4266.180	31351	(e)	2.5	54784	(o)	3.5	−3.45	−3.682	1.33E+05	7.15E−05
4269.272	31083	(e)	1.5	54499	(o)	1.5	−1.94	−2.167	4.32E+06	4.64E−03
4275.560	31117	(e)	2.5	54499	(o)	1.5	−1.47	−1.709	1.27E+07	1.37E−02
4284.190	31083	(e)	1.5	54418	(o)	0.5	−1.62	−1.864	8.79E+06	1.89E−02
4352.600	31531	(e)	1.5	54499	(o)	1.5	−3.66	−3.258	7.89E+04	8.48E−05
4368.107	31531	(e)	1.5	54418	(o)	0.5	−3.51	−3.015	1.09E+05	2.34E−04
4507.199	25047	(e)	2.5	47227	(o)	3.5	−3.94	−4.076	3.75E+04	1.92E−05
4539.590	32603	(e)	2.5	54626	(o)	2.5	−3.47	−2.530	1.10E+05	7.88E−05
4544.694	25043	(e)	1.5	47040	(o)	2.5	−3.98	−4.022	3.37E+04	2.36E−05
4558.787	32855	(e)	2.5	54784	(o)	3.5	−2.55	−2.462	8.89E+05	4.78E−04
4565.735	32603	(e)	2.5	54499	(o)	1.5	−2.99	−2.110	3.31E+05	3.56E−04
4588.198	32837	(e)	3.5	54626	(o)	2.5	−0.67	−0.630	6.55E+07	4.69E−02
4589.895	32845	(e)	1.5	54626	(o)	2.5	−2.45	−2.660	1.08E+06	7.74E−04
4592.052	32855	(e)	2.5	54626	(o)	2.5	−1.26	−1.220	1.69E+07	1.21E−02
4616.624	32845	(e)	1.5	54499	(o)	1.5	−1.40	−1.290	1.22E+07	1.31E−02
4618.807	32855	(e)	2.5	54499	(o)	1.5	−0.86	−1.110	4.17E+07	4.48E−02
4634.073	32845	(e)	1.5	54418	(o)	0.5	−1.05	−1.240	2.68E+07	5.76E−02
4713.969	33418	(e)	2.5	54626	(o)	2.5	−2.98	−3.559	3.09E+05	2.21E−04
4737.000	33521	(e)	3.5	54626	(o)	2.5	−2.30	−2.782	1.48E+06	1.06E−03
4742.167	33418	(e)	2.5	54499	(o)	1.5	−2.57	−3.125	7.94E+05	8.54E−04
4777.778	30864	(e)	2.5	51789	(o)	3.5	−3.97	−4.758	3.11E+04	1.59E−05
4805.200	30864	(e)	2.5	51669	(o)	2.5	−3.02	−4.583	2.76E+05	1.89E−04
4824.984	30864	(e)	2.5	51584	(o)	1.5	−3.80		4.51E+04	4.74E−05
4836.229	31117	(e)	2.5	51789	(o)	3.5	−1.87	−2.250	3.87E+06	1.98E−03
4856.190	31083	(e)	1.5	51669	(o)	2.5	−2.00	−2.260	2.84E+06	1.94E−03
4864.328	31117	(e)	2.5	51669	(o)	2.5	−1.31	−1.372	1.40E+07	9.57E−03
4876.397	31083	(e)	1.5	51584	(o)	1.5	−1.41	−1.457	1.09E+07	1.14E−02
4876.489	31169	(e)	3.5	51669	(o)	2.5	−1.89	−1.460	3.62E+06	2.47E−03
4884.603	31117	(e)	2.5	51584	(o)	1.5	−2.05	−2.080	2.53E+06	2.66E−03
4891.495	31351	(e)	2.5	51789	(o)	3.5	−3.54	−3.044	8.10E+04	4.15E−05
4920.242	31351	(e)	2.5	51669	(o)	2.5	−3.04	−2.488	2.52E+05	1.72E−04
4940.986	31351	(e)	2.5	51584	(o)	1.5	−3.63	−3.091	6.41E+04	6.73E−05
4985.413	31531	(e)	1.5	51584	(o)	1.5	−3.67	−3.932	5.67E+04	5.95E−05
5097.319	29952	(e)	0.5	49565	(o)	1.5	−3.04	−2.640	2.35E+05	2.47E−04
5116.047	29952	(e)	0.5	49493	(o)	0.5	−3.90	−3.630	3.26E+04	7.01E−05
5153.497	30307	(e)	1.5	49706	(o)	2.5	−2.72	−2.696	4.81E+05	3.61E−04
5191.434	30307	(e)	1.5	49565	(o)	1.5	−3.52	−3.362	7.53E+04	7.91E−05
5210.861	30307	(e)	1.5	49493	(o)	0.5	−3.20	−2.945	1.56E+05	3.35E−04
5246.117	35569	(e)	2.5	54626	(o)	2.5	−3.87	−4.167	3.38E+04	2.42E−05
5246.773	29952	(e)	0.5	49006	(o)	1.5	−2.57	−2.450	6.62E+05	7.78E−04
5249.435	30307	(e)	1.5	49352	(o)	2.5	−2.64	−2.426	5.60E+05	4.29E−04
5256.689	35608	(e)	3.5	54626	(o)	2.5	−3.23	−3.640	1.45E+05	1.04E−04
5267.029	32603	(e)	2.5	51584	(o)	1.5	−3.72	−3.324	4.56E+04	4.79E−05
5280.070	32855	(e)	2.5	51789	(o)	3.5	−2.17	−2.011	1.55E+06	7.94E−04
5281.065	35569	(e)	2.5	54499	(o)	1.5	−3.48	−3.863	8.03E+04	8.63E−05
5305.864	30864	(e)	2.5	49706	(o)	2.5	−2.40	−2.357	9.59E+05	7.19E−04
5308.421	32837	(e)	3.5	51669	(o)	2.5	−1.95	−1.810	2.52E+06	1.72E−03

(*continued on next page*)

Table 6 (*continued*)

Wavelength (Å)	E(Lower) (cm^{-1})	Parity (Lower)	J(Lower)	E(Upper) (cm^{-1})	Parity (Upper)	J(Upper)	log(gf)(HFR+CPOL)	log(gf) (Kurucz)	gA (HFR+CPOL) (s^{-1})	BF (HFR+CPOL)
5310.692	32845	(e)	1.5	51669	(o)	2.5	−2.29	−2.280	1.15E+06	7.86E−04
5313.581	32855	(e)	2.5	51669	(o)	2.5	−1.63	−1.650	5.31E+06	3.63E−03
5318.387	29952	(e)	0.5	48749	(o)	0.5	−3.28	−3.128	1.26E+05	3.15E−04
5334.868	32845	(e)	1.5	51584	(o)	1.5	−1.70	−1.562	4.40E+06	4.62E−03
5337.783	32855	(e)	2.5	51584	(o)	1.5	−2.12	−2.029	1.69E+06	1.77E−03
5346.086	30864	(e)	2.5	49565	(o)	1.5	−3.09	−2.650	1.93E+05	2.03E−04
5346.541	30307	(e)	1.5	49006	(o)	1.5	−3.09	−2.948	1.92E+05	2.26E−04
5378.048	31117	(e)	2.5	49706	(o)	2.5	−3.68	−4.400	4.90E+04	3.68E−05
5396.881	36102	(e)	3.5	54626	(o)	2.5	−3.60	−3.592	6.03E+04	4.32E−05
5407.615	30864	(e)	2.5	49352	(o)	2.5	−2.33	−2.088	1.08E+06	8.28E−04
5420.925	30307	(e)	1.5	48749	(o)	0.5	−2.61	−2.360	5.71E+05	1.43E−03
5441.898	33418	(e)	2.5	51789	(o)	3.5	−3.88	−4.260	2.90E+04	1.49E−05
5477.502	33418	(e)	2.5	51669	(o)	2.5	−2.89	−2.994	2.80E+05	1.91E−04
5503.224	33418	(e)	2.5	51584	(o)	1.5	−2.60	−2.306	5.33E+05	5.60E−04
5508.623	33521	(e)	3.5	51669	(o)	2.5	−2.48	−2.110	6.96E+05	4.76E−04
5510.718	30864	(e)	2.5	49006	(o)	1.5	−2.62	−2.452	5.30E+05	6.23E−04
5926.178	32837	(e)	3.5	49706	(o)	2.5	−4.00	−4.354	1.85E+04	1.39E−05
6070.107	38315	(e)	2.5	54784	(o)	3.5	−3.19	−2.944	1.10E+05	5.91E−05
6112.263	38270	(e)	3.5	54626	(o)	2.5	−3.14	−2.943	1.22E+05	8.74E−05
6129.226	38315	(e)	2.5	54626	(o)	2.5	−2.71	−2.440	3.29E+05	2.36E−04
6147.146	38362	(e)	1.5	54626	(o)	2.5	−3.08	−2.843	1.38E+05	9.89E−05
6176.982	38315	(e)	2.5	54499	(o)	1.5	−3.05	−2.841	1.49E+05	1.60E−04
6195.183	38362	(e)	1.5	54499	(o)	1.5	−3.04	−2.802	1.52E+05	1.63E−04
6208.189	38396	(e)	0.5	54499	(o)	1.5	−3.22	−2.984	9.97E+04	1.07E−04
6209.376	35569	(e)	2.5	51669	(o)	2.5	−3.99	−4.233	1.78E+04	1.22E−05
6226.645	38362	(e)	1.5	54418	(o)	0.5	−3.19	−2.981	1.04E+05	2.24E−04
6239.783	38396	(e)	0.5	54418	(o)	0.5	−3.22	−2.991	9.79E+04	2.10E−04
7419.668	38315	(e)	2.5	51789	(o)	3.5	−2.55	−2.424	3.15E+05	1.61E−04
7486.011	38315	(e)	2.5	51669	(o)	2.5	−3.15	−3.014	7.79E+04	5.32E−05
7512.760	38362	(e)	1.5	51669	(o)	2.5	−2.76	−2.630	1.90E+05	1.30E−04
7561.233	38362	(e)	1.5	51584	(o)	1.5	−3.30	−3.172	5.32E+04	5.59E−05
7580.615	38396	(e)	0.5	51584	(o)	1.5	−2.97	−2.838	1.15E+05	1.21E−04
18072.536	49352	(o)	2.5	54883	(e)	2.5	−3.92		2.38E+03	
52704.748	51669	(o)	2.5	53566	(e)	3.5	−3.99	−3.869	3.02E+02	
62420.503	51669	(o)	2.5	53271	(e)	2.5	−3.58	−3.492	5.75E+02	
68136.875	51584	(o)	1.5	53051	(e)	1.5	−3.70	−3.628	3.75E+02	
69034.463	53051	(e)	1.5	54499	(o)	1.5	−3.80	−3.673	2.03E+02	2.18E−07
73153.230	53051	(e)	1.5	54418	(o)	0.5	−3.46	−3.325	3.95E+02	8.49E−07
73803.061	53271	(e)	2.5	54626	(o)	2.5	−3.71	−3.577	2.22E+02	1.59E−07
81378.953	53271	(e)	2.5	54499	(o)	1.5	−3.31	−3.174	4.46E+02	4.79E−07
94372.311	53566	(e)	3.5	54626	(o)	2.5	−3.20	−3.057	4.32E+02	3.10E−07